CHEMISTRY
A EUROPEAN JOURNAL

DOI: 10.1002/chem.200903315

Hydrogels Composed of Organic Amphiphiles and α-Cyclodextrin: Supramolecular Networks of Their Pseudorotaxanes in Aqueous Media

Toshiaki Taira, Yuji Suzaki, and Kohtaro Osakada*[a]

Abstract: Mixtures of *N*-alkyl pyridinium compounds [py-*N*-$(CH_2)_n OC_6H_3$-3,5-$(OMe)_2$]$^+(X^-)$ (**1b**Cl: $n=10$, X = Cl; **1c**Br: $n=12$, X = Br) and α-cyclodextrin (α-CD) form supramolecular hydrogels in aqueous media. The concentrations of the two components influences the sol–gel transition temperature, which ranges from 7 to 67 °C. Washing the hydrogel with acetone or evaporation of water left the xerogel, and ^{13}C CP/MAS NMR measurements, powder X-ray diffraction (XRD), and scanning electron microscopy (SEM) revealed that the xerogel of **1b**Cl (or **1c**Br) and α-CD was composed of pseudorotaxanes with high crystallinity. $^{13}C\{^1H\}$ and ^1H NMR spectra of the gel revealed the detailed composition of the components. The gel from **1b**Cl and α-CD contains the corresponding [2]- and [3]pseudorotaxanes, [**1b**·(α-CD)]Br and [**1b**·$(\alpha\text{-CD})_2$]Br, while that from **1c**Br and α-CD consists mainly of [3]pseudorotaxane [**1c**·$(\alpha\text{-CD})_2$]Br. 2D ROESY ^1H NMR measurements suggested intermolecular contact of 3,5-dimethoxyphenyl and pyridyl end groups of the axle component. The presence of the [3]pseudorotaxane is indispensable for gel formation. Thus, intermolecular interaction between the end groups of the axle component and that between α-CDs of the [3]pseudorotaxane contribute to formation of the network. The supramolecular gels were transformed into sols by adding denaturing agents such as urea, C_6H_3-1,3,5-$(OH)_3$, and [py-*N*-*n*Bu]$^+(Cl^-)$.

Keywords: cyclodextrins · gels · micelles · rotaxanes · supramolecular chemistry

Introduction

Polysaccharides are among the important materials in terms of robust structure, rich functionality, and hydrophilicity.[1,2] Hydrogels composed of polysaccharides have low toxicity and potential applications in foods,[3] cosmetics processing and drug delivery,[4] tissue engineering,[5] and artificial molecular chaperones and catalysts.[6,7] Cyclodextrins (CDs), a series of cyclic oligosaccharides consisting of α-1,4-linked glucopyranose units, form cavities of different sizes depending on the number of glucose units.[8] Akashi et al. reported that channel-type aggregates of γ-CD form gels in organic solvents due to microcubic structure.[9] Although native CDs do not undergo gelation in water, host–guest complexes and polyrotaxanes of CDs form hydrogels. Harada and Kamachi reported that the polyrotaxane of α-CDs on polyethylene glycol (PEG, $M_w > 2000$) formed a physical gel in aqueous media.[10] Low occupancy of α-CDs on long PEG chains is necessary for aggregation of the polyrotaxanes and formation of the network structure. Direct bond formation between α-CDs in the polyrotaxane by condensation with cyanuric chloride resulted in a topological gel.[11,12] This new class of gel exhibits high tensile strength and large swellability due to cross-linking α-CDs.

Simple host–guest complexes containing CD also form gels in water. Gels formed from β-CD and pyridine are composed of their host–guest complex and free pyridine in 1:7 ratio.[13] The host–guest complexes of β-CD with polyaromatic hydrocarbons such as chrysene, anthracene, and triphenylene also form gels in DMF/H_2O.[14] Self-inclusion complexes of functionalized β-CDs exist as supramolecular polymers in water and form hydrogels.[15,16] [2]Rotaxanes and [4]pseudorotaxanes containing α-CD as the macrocyclic molecule form light-responsive hydrogels with *N*,*N*,*N*-trimethylhexadecan-1-aminium bromide and amphoteric surfactant as gelators.[17]

Here we report that pseudorotaxanes, simply obtained by mixing α-CD and common amphiphiles, form hydrogels with precisely controlled sol–gel phase transition temperature, and that [3]pseudorotaxanes play an essential role in

[a] T. Taira, Dr. Y. Suzaki, Prof. Dr. K. Osakada
Chemical Resources Laboratory
Tokyo Institute of Technology
4259 Nagastuta, Midori-ku, Yokohama 226-8503 (Japan)
Fax: (+81) 45-924-5224
E-mail: kosakada@res.titech.ac.jp

Supporting information for this article is available on the WWW under http://dx.doi.org/10.1002/chem.200903315.

gel formation. Part of this work was reported in a preliminary form.[18]

Results

Aggregation of amphiphiles in aqueous solution: Alkyl pyridinium compounds with a 3,5-dimethoxyphenyl group, [py-*N*-$(CH_2)_n$$OC_6H_3$-3,5-$(OMe)_2$]$^+X^-$ (**1a**Cl: $n=8$, X = Cl; **1b**Cl: $n=10$, X = Cl; **1c**Br: $n=12$, X = Br), were prepared by condensation of pyridine with $X(CH_2)_nOC_6H_3$-3,5-$(OMe)_2$ in DMF.[19] Exchange of the counteranion of **1b**Cl yielded [py-*N*-$(CH_2)_{10}OC_6H_3$-3,5-$(OMe)_2$]$^+X^-$ (**1b**NO_3: X = NO_3; **1b**PF_6: X = PF_6; **1b**[$PtCl_3$(dmso)]: X = $PtCl_3$(dmso), dmso = dimethyl sulfoxide).

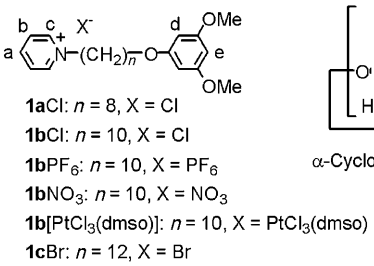

1aCl: n = 8, X = Cl
1bCl: n = 10, X = Cl
1bPF_6: n = 10, X = PF_6
1bNO_3: n = 10, X = NO_3
1b[$PtCl_3$(dmso)]: n = 10, X = $PtCl_3$(dmso)
1cBr: n = 12, X = Br

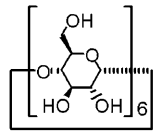

α-Cyclodextrin (α-CD)

Amphiphilic compounds **1a**Cl, **1b**Cl, and **1c**Br are expected to form micelles in aqueous solution.[20] Aggregation of **1b**Cl and α-CD in aqueous solution has been examined in the presence of hydrophobic pigments such as Nile red ($\lambda_{max}=577$ nm) and pyrene ($\lambda_{max}=338$ nm).[21,22] Dissolution of **1b**Cl and Nile red ([Nile red]$_0=10$ μM) in water leads to aggregation of **1b**Cl to form micelles that encapsulate Nile red molecules in the core. Figure 1a shows absorption spectra of solutions with different concentration of **1b**Cl (from 3.1×10^{-6} to 1.0×10^{-2} g mL^{-1}). The solution of **1b**Cl below 6.3×10^{-5} g mL^{-1} shows peaks at 526 and 577 nm, but increasing the concentration above 6.4×10^{-4} g mL^{-1} causes significant increase of the peak at 577 nm, which is assigned to dye encapsulated within micelles. The critical micelle concentration (CMC) of **1b**Cl was determined to be 6.4×10^{-4} g mL^{-1} (1.6 mM) at 25 °C on the basis of plots of absorbance at 577 nm versus [**1b**Cl] (Figure 1b). The CMCs of **1a**Cl and **1c**Br were similarly determined to be 3.9 and 0.5 mM, respectively. The emission spectrum of the aqueous solution containing **1b**Cl (2.0 mM) and pyrene (5.0 μM) shows the peak corresponding to pyrene (Figure 2). The

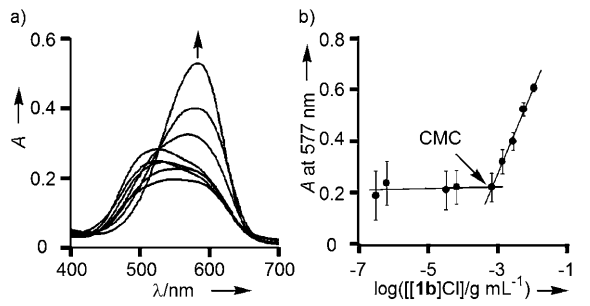

Figure 1. a) Absorption spectra of aqueous solutions of Nile red and **1b**Cl with various concentrations of **1b**Cl (from 3.1×10^{-6} to 1.0×10^{-2} g mL^{-1}). b) Plots of absorbance at 577 nm versus concentration of **1b**Cl.

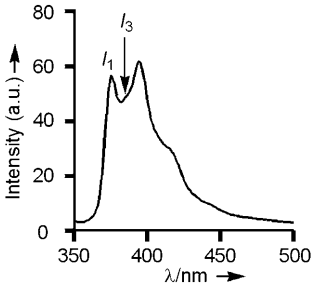

Figure 2. Emission spectrum of 2.0 mM **1b**Cl and 5.0 μM pyrene (H_2O, RT, $\lambda_{ex}=333$ nm).

ratio of the I_1 (375 nm) and the I_3 (385 nm) peaks of pyrene monomer, $I_3/I_1=0.86$, indicates that the pyrene is located in a nonpolar microenvironment.[22]

We also investigated the micelle-formation process of **1b**Cl in D_2O using ^{1}H NMR spectroscopy (Figure 3). In-

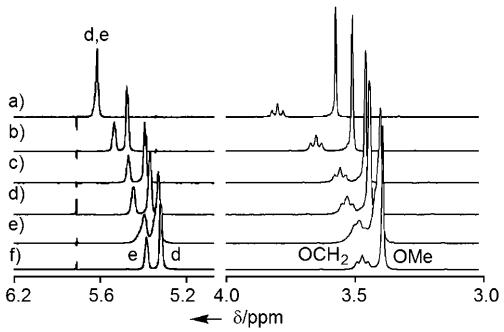

Figure 3. ^{1}H NMR spectrum of **1b**Cl (D_2O, RT) at a) 5.0 mM, b) 10 mM, c) 20 mM, d) 30 mM, e) 40 mM, and f) 50 mM.

creasing concentration of **1b**Cl from 5.0 to 50 mM causes upfield shifts of the signals. Signal e of *para*-C_6H_3-3,5-$(OMe)_2$ at 5.0 mM shows a large shift and overlaps with the signal d ($\delta=-0.35$ ppm) at higher concentration, whereas CH_2 peaks close to the pyridinium group show much smaller changes in peak position (<0.07 ppm). These results indicate that the dimethoxyphenyl groups are located inside the micelle particle and may interact with aromatic dye or with each other. Changes in peak positions depending on concentration of **1b**Cl indicate that **1b**Cl in the micelle particle undergoes fast exchange with that in solution or with that in other micelle particles above the NMR timescale. Addition of α-CD to a micellar solution of **1b**Cl and pyrene ([**1b**Cl] = 12.3 mM, [pyrene] = 10 μM) at 25 °C decreased absorption depending on the amount of α-CD. Figure 4 shows the de-

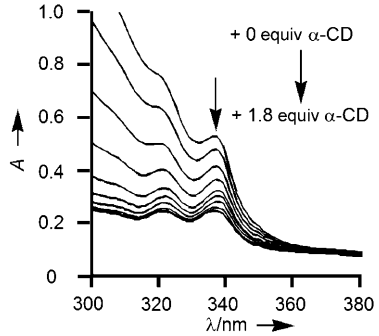

Figure 4. Absorption spectra of **1b**Cl and pyrene ([**1b**Cl] = 12.3 mM, [pyrene] = 10 μM) in aqueous solutions with various concentrations of α-CD [from 0 (0 equiv) to 22.1 mM (1.8 equiv)].

crease of the absorbance at 338 nm from 0.52 to 0.24 caused by addition of α-CD. These results are ascribed to the fact that the encapsulated pyrene in the micelle is released from the core by ready formation of [2]- and [3]pseudorotaxanes [**1b**•(α-CD)] and [**1b**•(α-CD)$_2$]Cl with α-CD. Host–guest complexation of the amphiphile and CD was reported by many groups,[23] and regarded as complexation controlled by external stimulus.[20,24]

Pseudorotaxane formation in solution: Scheme 1 summarizes equilibria among the amphiphiles (**1a**Cl, **1b**Cl, **1c**Br) and

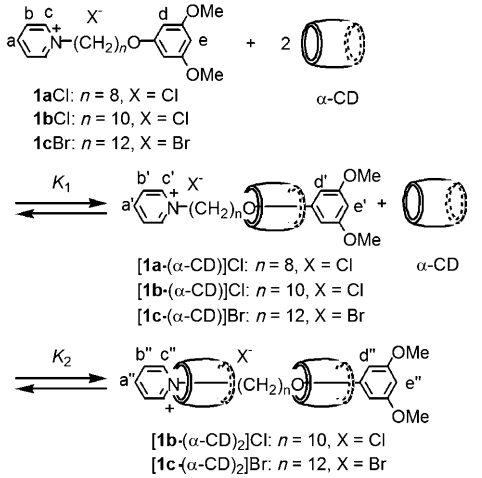

Scheme 1. Formation of [2]- and [3]pseudorotaxanes in aqueous solution. Isomers of [2]- and [3]pseudorotaxane are omitted.

their [2]- and [3]pseudorotaxanes with α-CD in aqueous media.[25,26] The ^{1}H NMR spectra of a mixture of the alkyl pyridinium compound and α-CD at low concentration (< 10 mM) confirmed the presence of pseudorotaxanes. Hydrogen atoms in the *ortho* positions of the aryl group of **1c**Br, [**1c**•(α-CD)]Br, and [**1c**•(α-CD)$_2$]Br give rise to the corresponding signals at $\delta = 5.74$, 6.06 (and a minor peak at $\delta =$ 6.14) and 5.63 ppm, respectively. Job plots of the peak of the aromatic end group of the mixtures of **1c**Br and α-CD with different molar ratios showed a maximum at a molar fraction close to 0.50, which indicates 1:1 complexation of α-CD and **1c**Br to form [**1c**•(α-CD)]Br (Figure 5a and bi). The

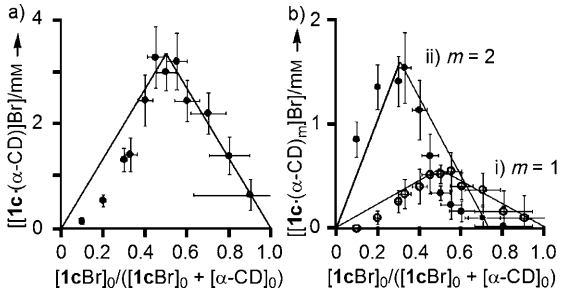

Figure 5. Job plots of a) [[**1c**•(α-CD)]Br] obtained from ^{1}H NMR peak area of d′, b) [[**1c**•(α-CD)$_m$]Br] obtained from ^{1}H NMR area of i) d′(*) ($m = 1$) and ii) d″ ($m = 2$) The concentrations were obtained by means of ^{1}H NMR area ratios of d, d′, d′(*), and d″. Sum of the concentrations of the two components was fixed to 10 mM in all cases.

plot obtained from peak d″ shows a maximum close to a molar fraction of 0.33 (Figure 5bii), which indicates that **1c**Br and α-CD form not only the [2]pseudorotaxane but also [3]pseudorotaxane [**1c**•(α-CD)$_2$]Br.

^{1}H and ^{13}C{^{1}H} NMR spectra and MALDI-TOF mass spectra of the D_2O solution of **1a**Cl and α-CD indicate the formation of [2]pseudorotaxane [**1a**•(α-CD)]Cl rather than the [3]pseudorotaxane. Association constants for formation of the pseudorotaxanes $K_1 =$ [[2]pseudorotaxane]/([*N*-alkyl pyridinium][α-CD] and $K_2 =$ [[3]pseudorotaxane]/([[2]pseudorotaxane][α-CD]) were obtained by comparison of ^{1}H NMR peak area ratio of the other hydrogen signals. The van't Hoff plots of K_1 and K_2 (Scheme 1) provided thermodynamic parameters for formation of [2]pseudorotaxanes (ΔH_1° and ΔS_1°) and [3]pseudorotaxanes (ΔH_2° and ΔS_2°), respectively, as listed in Table 1. A mixture of **1a**Cl and α-CD forms a stable [2]pseudorotaxane with a large equilibrium constant, $K_1 = 2.8 \times 10^3\,\text{M}^{-1}$ at 298 K, although [3]pseudorotaxane is not observed in the mixtures. Formation of both [2]- and [3]pseudorotaxanes of α-CD with **1b**Cl ($K_1 = 5.3 \times 10^2\,\text{M}^{-1}$, $K_2 = 30\,\text{M}^{-1}$) is less favorable than that with **1c**Br ($K_1 = 1.7 \times 10^3\,\text{M}^{-1}$, $K_2 = 2.1 \times 10^2\,\text{M}^{-1}$).

The thermodynamic parameters in Table 1 suggest thermodynamically favorable pseudorotaxane formation under enthalpy control. The negative enthalpy change of [2]pseu-

Table 1. Thermodynamic parameters for formation of [2]pseudorotaxane (K_1, ΔH_1°, ΔS_1°, and ΔG_1°) and [3]pseudorotaxane (K_2, ΔH_2°, ΔS_2°, and ΔG_2°) at 298 K.

Axle	K_1 (K_2) [M^{-1}]	ΔH_1° [ΔH_2°] [kJ mol^{-1}]	ΔS_1° [ΔS_2°] [J K^{-1} mol^{-1}]	ΔG_1° [ΔG_2°] [kJ mol^{-1}]
1aCl	2.8×10^3 (–)	−37(2) [–]	−58(7) [–]	−20(5) [–]
1bCl	5.3×10^2 (30)	−24(2)	−27(6)	−16(4)
		[−77(7)]	[$-2.3(2) \times 10^2$]	[−8(13)]
1cBr	1.7×10^3	−19(1)	−3(3)	−18(2)
	(2.1×10^2)	[−47(5)]	[$-1.1(2) \times 10^2$]	[−13(10)]

dorotaxane formation, ΔH_1°, is attributed to the hydrophobic interaction between α-CD and the axle molecule. The larger negative value of ΔH_2° compared to ΔH_1° suggests a contribution of hydrogen-bonding interactions between OH groups of two α-CDs in the [3]pseudorotaxane.[27]

The dependence of ΔS_1° on the chain length of the axle moiety can be explained by solvation and the bent structure due to intramolecular π–π interaction of the axle unit (vide infra).[28] The enthalpy–entropy compensation plot ($\Delta H°$ vs. $T\Delta S°$) for pseudorotaxane formation gave a straight line with a slope of 1.2(1) and an intercept of 22(3) kJ mol^{-1} (see Supporting Information). These values are larger than those of the inclusion equilibrium of α-CD with a variety of small guest molecules;[29] the slope (0.79) and the intercept (8.0 kJ mol^{-1}) suggest that pseudorotaxane formation in our study involves significant conformational change and extensive desolvation due to the large guest molecules. A 2D ROESY ^{1}H NMR cross-peak of the protons in the 3-position of α-CD (H3) and C_6H_3 proton of [**1a**•(α-CD)]Cl (e′) indicates [2]pseudorotaxane formation in which primary hydroxyl groups of α-CD face the C_6H_3-3,5-$(OMe)_2$ moiety (Figure 6). The 2D ROESY ^{1}H NMR spectrum of [**1b**•(α-CD)]Cl exhibits cross-peaks of NCH_2 proton of **1b** with H atoms of α-CD, H5 and H6, that is, α-CD is located on the polymethylene group of [**1b**•(α-CD)]Cl.[30–32] These solutions do not form hydrogels under the conditions examined.

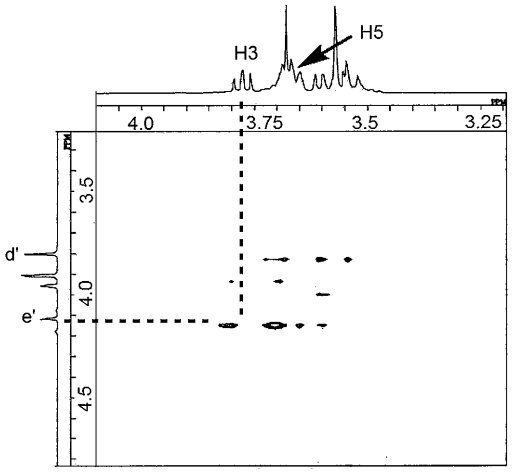

Figure 6. 2D ROESY NMR spectrum (D_2O, 30 °C) of **1a**Cl (20 mM) and α-CD (20 mM).

Gelation of *N*-alkyl pyridinium and α-CD: Amphiphilic compounds **1a**Cl, **1b**Cl, and **1c**Br form micelles in aqueous solution (vide infra) and do not form hydrogels even at high concentration. Addition of α-CD (100 mM) to an aqueous solution containing 50 mM of **1b**Cl or **1c**Br at 60 °C and cooling it to room temperature yields hydrogels (Figure 7b, c), while mixtures of α-CD and alkyl pyridinium with a shorter polymethylene chain (**1a**Cl, $n=8$) do not form hydrogels under the same conditions (Figure 7a).

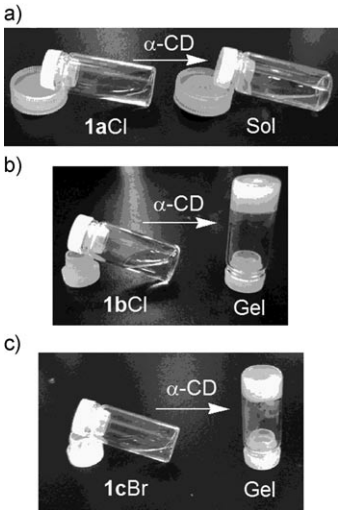

Figure 7. Photographs. a) Left: **1a**Cl (50 mM); right: **1a**Cl (50 mM) and α-CD (100 mM) (sol). b) Left: **1b**Cl (50 mM); right: **1b**Cl (50 mM) and α-CD (100 mM) (gel). c) Left: **1c**Br (50 mM); right: **1c**Br (50 mM) and α-CD (100 mM) (gel).

Figure 8 depicts the relationship between the gel-to-sol phase transition temperature T_{gel} and concentration of the components. Mixtures of **1b**Cl and α-CD in water show T_{gel} ranging from 7 °C ([**1b**Cl] = 60 mM, [α-CD] = 60 mM) to 32 °C

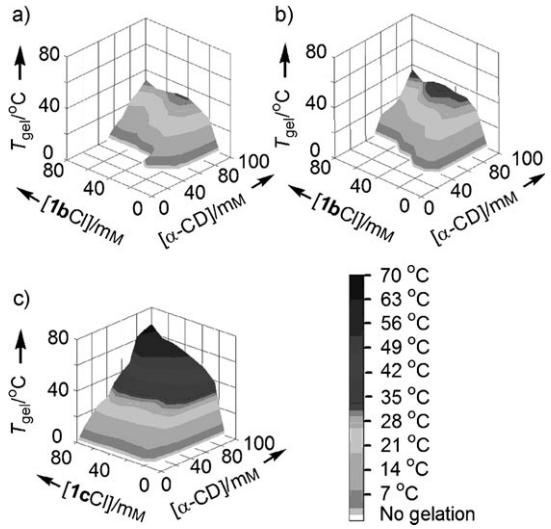

Figure 8. Phase-transition temperature T_{gel} at various concentrations of a) **1b**Cl and α-CD in H_2O, b) **1b**Cl and α-CD in D_2O, and c) **1c**Br and α-CD in H_2O.

([**1b**Cl] = 80 mM, [α-CD] = 100 mM), as shown in Figure 8a. The mixture shows higher T_{gel} in D_2O, ranging from 12 °C ([**1b**Cl] = 50 mM, [α-CD] = 50 mM) to 36 °C ([**1b**Cl] = 80 mM, [α-CD] = 100 mM), than in H_2O (Figure 8b). The hydrogel of a mixture of **1c**Br and α-CD is thermally more stable than that of **1b**Cl and α-CD at the same concentration, and T_{gel} attains 67 °C ([**1c**Br] = 80 mM, [α-CD] = 100 mM; Figure 8c). Table 2 summarizes the effect of the counter ion X^-

Table 2. Gelation properties of *N*-alkyl pyridinium compounds and CDs in H_2O.

System[a]	State[b]	T_{gel} [°C]
α-CD + **1a**Cl	sol	–
α-CD + **1b**Cl	gel	32(1), 35(1)[c]
α-CD + **1b**NO_3	gel	35(1)
α-CD + **1b**PF_6	insol	–
α-CD + **1b**[$PtCl_3$(dmso)]	sol	–
α-CD + **1c**Br	gel	50(1)
β-CD + **1b**Cl	sol	–
γ-CD + **1b**Cl	sol	–

[a] [*N*-alkyl pyridinium] = 50 mM, [CD] = 100 mM. [b] Gel: gelation, insol: insoluble, sol: solution. [c] T_{gel} in D_2O.

on gelation of a mixture of **1b**X (50 mM) and α-CD (100 mM). The T_{gel} of **1b**NO_3 (35 °C) is higher than that of **1b**Cl (32 °C). Amphiphile **1b**PF_6 is not soluble in water, and its mixture with α-CD does not form a hydrogel. Water-insoluble **1b**[$PtCl_3$(dmso)] dissolves upon addition of α-CD at 60 °C to give a clear solution of their inclusion complex. β-CD and γ-CD do not gelate **1b**Cl in water.

A xerogel of **1b**Cl (**1c**Br) and α-CD (1:2) was obtained by slow evaporation of water from the hydrogel or by washing the hydrogel with acetone. The following results indicate that the xerogels are composed of pseudorotaxanes of the above compounds. The MALDI-TOFMS spectrum of the xerogel of **1b**Cl/α-CD contains peaks at *m*/*z* 1344.6 and 2316.7, which correspond to [2]pseudorotaxane [{py-*N*-$(CH_2)_{10}OC_6H_3$-3,5-$(OMe)_2$}(α-CD)]$^+Cl^-$ ([**1b**•(α-CD)]Cl) and [3]pseudorotaxane [{py-*N*-$(CH_2)_{10}OC_6H_3$-3,5-$(OMe)_2$}-$(\alpha\text{-CD})_2$]$^+Cl^-$ ([**1b**•$(\alpha\text{-CD})_2$]Cl), respectively. The xerogel obtained from **1c**Br and α-CD also shows peaks assigned to their [2]- and [3]pseudorotaxanes (*m*/*z* 1373.4 and 2347.6).

Figure 9 compares the ^{13}C CP/MS NMR spectra of α-CD, the xerogel of **1c**Br/α-CD, and **1c**Br. The signals of the alkyl pyridinium group in the xerogel are broadened significantly (Figure 9b), if compared with free **1c**Br (Figure 9c). The C1 and C4 carbon atoms of free α-CD are observed as multiple peaks (δ = 81, 98 ppm) due to the strained glycosidic linkage

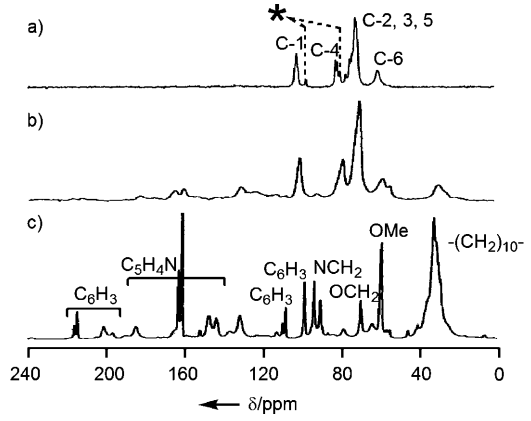

Figure 9. ^{13}C CP/MS NMR spectra (100 Hz, RT) of a) α-CD, b) Xerogel of **1c**Br and α-CD, and c) **1c**Br. Peaks with an asterisk are assigned to C1 and C4 with a conformationally strained glycosidic linkage.

and low-symmetry conformation of the macrocyclic compound (peaks with asterisk in Figure 9a).[33] The xerogel does not exhibit the corresponding signals, that is, α-CD in the xerogel adopts a symmetrical cyclic conformation similar to other host–guest compounds and rotaxanes of α-CD (Figure 9b, c). These NMR results also indicate that the xerogel is composed of pseudorotaxanes. The powder X-ray diffraction (XRD) patterns of the xerogels of **1b**Cl/α-CD and of **1c**Br/α-CD show diffraction peaks at 2θ = 5.5, 10.9° (Figure 10a) and 2θ = 5.7, 11.2° (Figure 10b), respectively. They

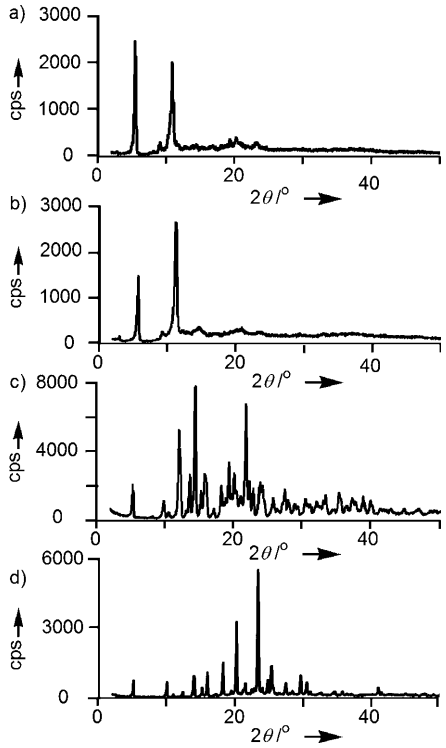

Figure 10. X-ray diffraction patterns ($Cu_{K\alpha}$, RT) of xerogels of a) **1b**Cl and α-CD, b) **1c**Br and α-CD, c) α-CD, d) **1b**Cl.

can be assigned to {001} and {002} diffraction of the columnar alignment of the α-CD moiety of the pseudorotaxanes.[34] These diffraction peaks were not observed in the patterns of α-CD and of **1b**Cl (Figure 10c, d). Scanning electron microscopy (SEM) of the xerogel revealed sheetlike layer morphology, as shown in Figure 11.[35]

Pseudorotaxane formation on hydrogelation: Figure 12 shows changes in the $^{13}C\{^1H\}$ NMR spectra of **1a**Cl, **1b**Cl and **1c**Br upon addition of α-CD in D_2O. A solution of a mixture of **1a**Cl (2.0×10^2 mM) and α-CD (4.0×10^2 mM) gives rise to signals of C3 and C2 due to [2]pseudorotaxane [**1a**•(α-CD)]Cl (δ = 76.5 and 74.4 ppm) (Figure 12a, bottom). The $^{13}C\{^1H\}$ NMR spectrum of a mixture of **1b**Cl (50 mM) and α-CD (50 mM) exhibits signals assigned to C3, C5, and C2 of [2]pseudorotaxane [**1b**•(α-CD)]Cl at δ = 76.5, 74.5, and 74.2 ppm, exclusively (Figure 12b, middle). Further addition of α-CD to the solution leads to hydrogelation, and its spec-

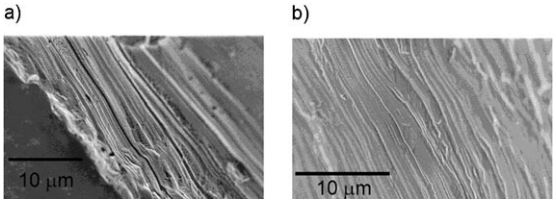

Figure 11. SEM image of xerogels of a) **1b**Cl/α-CD, b) **1c**Br/α-CD.

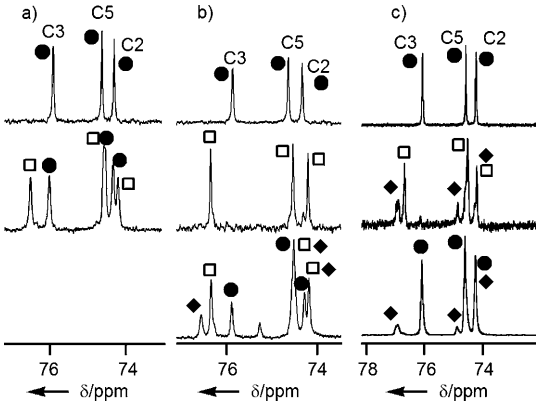

Figure 12. $^{13}C\{^1H\}$ NMR spectra (D_2O, RT) of a) α-CD (top) and a mixture of **1a**Cl (2.0×10^2 mM) and α-CD (4.0×10^2 mM) (bottom). b) α-CD (top), a mixture of **1b**Cl (50 mM) and α-CD (50 mM) (middle), and a mixture of **1b**Cl (50 mM) and α-CD (1.0×10^2 mM) (gel) (bottom). c) α-CD (top), a mixture of **1c**Br (20 mM) and α-CD (20 mM) (gel) (middle), and a mixture of **1c**Br (20 mM) and α-CD (90 mM) (gel) (bottom). (●: α-CD, □: [2]pseudorotaxane, ◆: [3]pseudorotaxane).

trum contains C3 signals of [3]pseudorotaxane [**1b**·(α-CD)$_2$]Cl ($\delta=76.7$ ppm; Figure 12b, bottom). A mixture of **1c**Br and α-CD forms hydrogel even at low concentration (20 mM) in D_2O. $^{13}C\{^1H\}$ NMR signals of both [2]- and[3]-pseudorotaxanes are observed (Figure 12c, middle). Further addition of α-CD converts [**1c**·(α-CD)]Br to [**1c**·(α-CD)$_2$]Br, giving a mixture of the [3]pseudorotaxane and free α-CD (Figure 12c, bottom).

Figure 13 compares the ^1H NMR spectra of **1c**Br and mixtures of **1c**Br and α-CD ([**1c**Br]=20 mM, [α-CD]=10–195 mM). The solution containing **1c**Br (20 mM) and α-CD (10 mM) shows signals of **1c**Br as well as a set of peaks due to [**1c**·(α-CD)]Br at $\delta=8.39$ (a′), 7.91 (b′), 6.10 (e′), 6.06 (d′) and 1.94 ppm (f′) (Figure 13ii). These peaks are at different positions than those of **1c**Br ($\delta=8.42$ (a), 7.49 (b), 5.79 (d), 5.74 (e), 1.75 ppm (f)). Further addition of α-CD ([**1c**Br]= 20 mM, [α-CD]=20–30 mM) increases the amount of [**1c**·(α-CD)]Br and generates [3]pseudorotaxane [**1c**·(α-CD)$_2$]Br with a new set of signals at $\delta=8.47$ (a″), 7.99 (b″), 6.17 (e″), 5.63 (d″), and 1.85 ppm (f″). Small signals at $\delta=6.14$ [d′(*)], 6.11 [e′(*)] and 1.87 ppm [f′(*)] may be attributed to an isomer of [**1c**·(α-CD)]Br with different orientation of the α-CD on the alkylene group.

Figure 13v–x show the ^1H NMR spectra at higher concentrations of α-CD ([α-CD]≥40 mM), and the D_2O solution turned to hydrogel under these conditions. The signals of the NMR spectra correspond to molecules entrapped in the space in the gel network. The molecules of **1c**Br contained in the network may not show the clear sharp NMR signals due to restricted molecular motion and much longer relaxation time of the nuclei. Signals of the NCH_2CH_2 hydrogen atoms of [**1c**·(α-CD)$_2$]Br [f″ and f″(*)] are observed at $\delta=$ 1.74–2.00 ppm as two broadened signals, although they severely overlap with the signals of [**1c**·(α-CD)]Br [f′ and f′(*)]. They indicate the existence of isomers of [**1c**·(α-

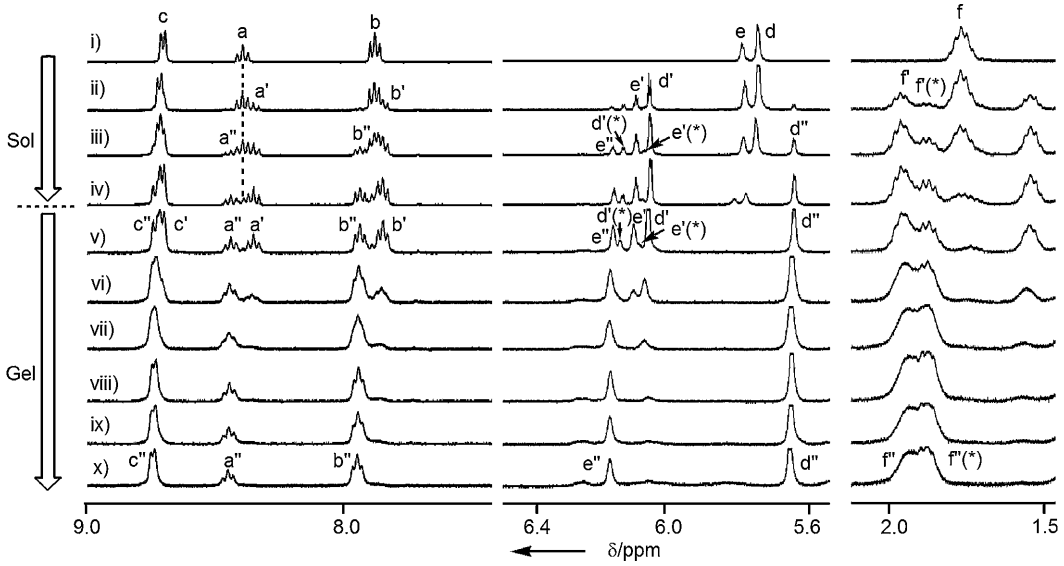

Figure 13. ^1H NMR spectra (D_2O, 25°C) of i) **1c**Br (20 mM), ii) a mixture of **1c**Br and α-CD ([**1c**Br]$_0$=20 mM, [α-CD]$_0$=10 mM), iii) a mixture of **1c**Br and α-CD ([**1c**Br]$_0$=20 mM, [α-CD]$_0$=20 mM), iv) a mixture of **1c**Br and α-CD ([**1c**Br]$_0$=20 mM, [α-CD]$_0$=30 mM), v) a mixture of **1c**Br and α-CD ([**1c**Br]$_0$=20 mM, [α-CD]$_0$=40 mM) (Gel), vi) a mixture of **1c**Br and α-CD ([**1c**Br]$_0$=20 mM, [α-CD]$_0$=50 mM) (gel), vii) a mixture of **1c**Br and α-CD ([**1c**Br]$_0$=20 mM, [α-CD]$_0$=65 mM) (gel), viii) a mixture of **1c**Br and α-CD ([**1c**Br]$_0$=20 mM, [α-CD]$_0$=85 mM) (gel), ix) a mixture of **1c**Br and α-CD ([**1c**Br]$_0$=20 mM, [α-CD]$_0$=115 mM) (gel), and x) a mixture of **1c**Br and α-CD ([**1c**Br]$_0$=20 mM, [α-CD]$_0$=195 mM) (gel).

CD)$_2$]Br with regard to orientation of two α-CDs.[27,30,31] Figure 13viii–x ([α-CD] ≥ 85 mM) contain almost negligible signals of [**1c**•(α-CD)]Br and large signals of [3]pseudorotaxane [**1c**•(α-CD)$_2$]Br. Since [3]pseudorotaxane [**1c**•(α-CD)$_2$]Br dissolved within the gel network undergoes exchange with the rotaxanes contained in the network, the gel network is probably composed mainly of the [3]pseudorotaxane. Mixtures of **1b**Cl and α-CD in D_2O also show ^{1}H NMR signals of [2]- and [3]pseudorotaxanes [**1b**•(α-CD)]Cl and [**1b**•(α-CD)$_2$]Cl.[18]

Figure 14 plots concentrations of the compounds existing in solution and gel as a function of temperature. The mixture ([**1c**Br] = 20 mM, [α-CD] = 1.0×10^2 mM) in D_2O forms a

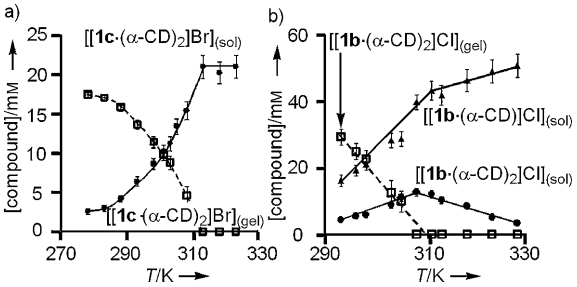

Figure 14. Temperature-dependent change of a) [[**1c**•(α-CD)$_2$]Br$_{(gel)}$] (□) and [[**1c**•(α-CD)$_2$]Br$_{(sol)}$] (●), b) [[**1b**•(α-CD)$_m$]Cl$_{(gel)}$] (□) (m = 1, 2), and [[**1b**•(α-CD)]Cl$_{(sol)}$] (▲), and [[**1b**•(α-CD)$_2$]Cl$_{(sol)}$] (●). Concentration of the compounds in gel was estimated from that in solution.

hydrogel at 5 °C (278 K) showing broadened ^{1}H NMR signals assigned to [**1c**•(α-CD)$_2$]Br$_{(sol)}$ dissolved in entrapped water in hydrogel with on concentration of 2.6 mM. Raising the temperature increases the amount of [**1c**Br•(α-CD)$_{2(sol)}$] and decreases that of [**1c**•(α-CD)$_2$]Br$_{(gel)}$] (concentration of [**1c**•(α-CD)$_2$]Br incorporated into the hydrogel network), as shown in Figure 14a. The ^{1}H NMR signals of [**1c**•(α-CD)]Br or **1c**Br are not observed in the range 278–323 K. Hydrogel formed from **1b**Cl and α-CD ([**1b**Cl] = 50 mM, [α-CD] = 1.0×10^2 mM) contains [**1b**•(α-CD)]Cl and [**1b**•(α-CD)$_2$]Cl, whose concentration varies depending on temperature (Figure 14b).

Equilibria of [2]- and [3]pseudorotaxanes in the gel and in aqueous solution are shown in Scheme 2:[14,36–38] The [2]- and [3]pseudorotaxanes are equilibrated in solution, as shown in Schemes 1 and 2. The dissolution equilibrium constants K_{d1} and K_{d2} can be defined as K_{d1} = [[2]pseudorotaxane$_{(sol)}$] and K_{d2} = [[3]pseudorotaxane$_{(sol)}$] by assuming activity of the gel to be unity, which allows estimation of thermodynamic parameters for gelation and dissolution, ΔH°_d and ΔS°_d from the plots of lnK_d versus 1/T. Figure 15 plots lnK_d against 1/T.

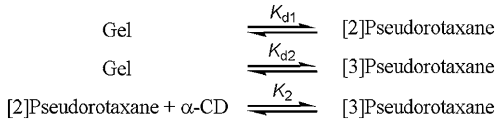

Scheme 2. Equilibria of [2]- and [3]pseudorotaxanes.

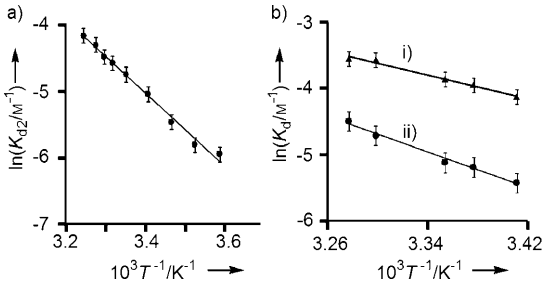

Figure 15. Plots of lnK_d versus 1/T for a) **1c**Br•(α-CD)$_2$ and b) i) **1b**Cl•(α-CD) and ii) **1b**Cl•(α-CD)$_2$.

Gelation of [**1c**•(α-CD)$_2$]Br$_{(sol)}$ and dissolution of [**1c**•(α-CD)$_2$]Br$_{(gel)}$ occur reversibly. Temperature dependence of K_{d2}, which was estimated to be [**1c**Br•(α-CD)$_{2(sol)}$], gave $\Delta H^\circ_{d2} = 45(2)$ kJ mol^{-1}, $\Delta S^\circ_{d2} = 1.1(1)\times10^2$ J K^{-1} mol^{-1} and $\Delta G^\circ_{d2} = 12(3)$ kJ mol^{-1} (Figure 15a). Equilibrium constant K_{d1} was also equal to [**1b**Cl•(α-CD)$_{(sol)}$], and the thermodynamic parameters were obtained from the van't Hoff plots (Figure 15b), giving $\Delta H^\circ_{d1} = 37(3)$ kJ mol^{-1}, $\Delta S^\circ_{d1} = 93(9)$ J K^{-1} mol^{-1}, and $\Delta G^\circ_{d1} = 10(5)$ kJ mol^{-1}. Dissolution of the [3]pseudorotaxane in gel occurs with thermodynamic parameters $\Delta H^\circ_{d2} = 57(4)$ kJ mol^{-1}, $\Delta S^\circ_{d2} = 1.5(1)\times10^2$ J K^{-1} mol^{-1}, and $\Delta G^\circ_{d2} = 13(7)$ kJ mol^{-1} (Figure 15b ii).

Chemical response of hydrogel: Figure 16 summarizes formation of hydrogel from **1b**Cl and α-CD and transformation to sol induced by addition of guest molecules. The hydrogel composed of **1b**Cl and α-CD ([**1b**Cl] = 50 mM, [α-CD] = 100 mM, T_{gel} = 32 °C, Figure 16i, ii) is turned into low-viscosity suspension by addition of an excess of NaCl (500 mM) (Figure 16ii, iii). Gel-to-sol phase transition is caused by addition of 200 mM of urea or phloroglucinol (Figure 16iv, v). Addition of C_6H_3-1,3,5-(OH)$_3$ (200 mM) to a D_2O solution of **1b**Cl and α-CD did not change the ^{1}H NMR and the 2D

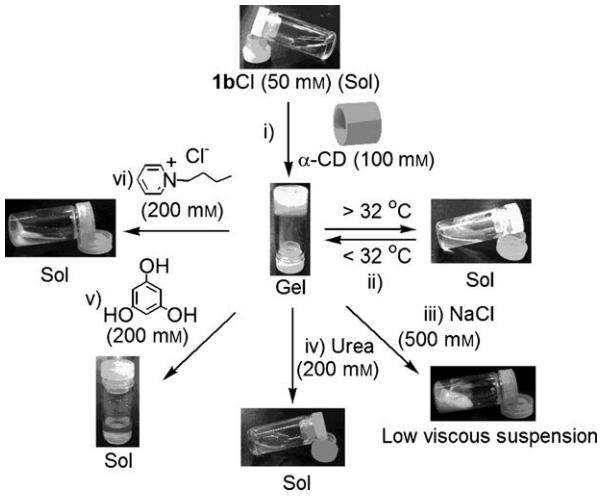

Figure 16. Illustration and photograph of thermally and chemically responsive properties of hydrogel of **1b**Cl and α-CD ([**1b**Cl] = 50 mM, [α-CD] = 100 mM).

ROESY ^{1}H NMR spectra. The 2D ROESY ^{1}H NMR spectrum of the solution containing **1b**Cl (50 mM), α-CD (100 mM), and C_6H_3-1,3,5-$(OH)_3$ (200 mM) shows an ROE correlation between NCH_2 and C_6H_3 protons of [2]- and [3]pseudorotaxanes of **1b**Cl and α-CD, which indicates that the pseudorotaxane structure and interpseudorotaxane interaction between C_6H_3-3,5-$(OMe)_2$ and the pyridyl moiety are also maintained in the sol. Addition of [py-*N*-*n*Bu]$^+$(Cl^-) (200 mM) to the hydrogel leads to gel-to-sol phase transition (Figure 16v, vi). The results suggest that interaction of cationic [py-*N*-*n*Bu]$^+$(Cl^-) with the electron-rich C_6H_3-3,5-$(OMe)_2$ group of the rotaxanes degrades the supramolecular polymers of the pseudorotaxanes.[39]

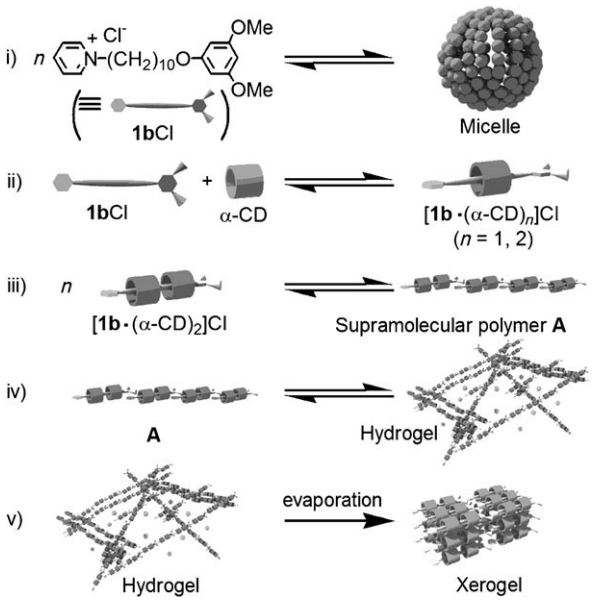

Figure 17. Plausible mechanism for formation of the supramolecular hydrogel.

Discussion

Figure 17 summarizes a plausible gelation mechanism. Compound **1b**Cl forms micelles above the CMC (Figure 17i). Addition of α-CD to the micellar solution of **1b**Cl forms [2]pseudorotaxane [**1b**·(α-CD)]Cl. It does not form micelles due to less significant intermolecular interaction of the alkyl chains complexed with α-CD than those without the pseudorotaxane structure (Figure 17ii). Further reaction of α-CD with [2]pseudorotaxane leads to formation of [3]pseudorotaxane [**1b**·$(\alpha\text{-CD})_2$]Cl. The thus-formed [**1b**·$(\alpha\text{-CD})_2$]Cl and [**1b**·(α-CD)]Cl aggregate to form supramolecular polymer **A** through attractive interaction between C_6H_3-3,5-$(OMe)_2$ and pyridyl moieties, which is observed by ROESY experiments (Figure 17iii). Further aggregation of **A** results in hydrogelation (Figure 17iv). Evaporation of water from the hydrogel yields a xerogel composed of [**1b**·$(\alpha\text{-CD})_m$]Cl ($m = 1,2$) (Figure 17v). The solid state is maintained by hydrogen bonds between α-CDs and channel-type packing yielding the layer morphology, which are observed by XRD and SEM analysis. This hydrogen bonding between α-CDs and formation of microcrystals may be important for cross-linking of supramolecular polymer **A** in the hydrogel (Figure 17v). Addition of urea, C_6H_3-1,3,5-$(OH)_3$, or [py-*N*-*n*Bu]$^+$(Cl^-) to the hydrogel causes transition of gel to sol. C_6H_3-1,3,5-$(OH)_3$ cleaves the cross-links of the gel network, in which the pseudorotaxane remains as the supramolecular polymer. Stacking of [py-*N*-*n*Bu]$^+$(Cl^-) with $C_6H_3(OMe)_2$ groups leads to degradation of the supramolecular polymer and results in phase transition to sol.

Figure 18 summarizes the energy diagram of the hydrogelation of **1c**Br and α-CD. Although each step involves a negative change of entropy due to multicomponent complexation, formation of hydrogel is a thermodynamically favorable reaction ($\Delta G_{(total)} = -43(15)$ kJ mol^{-1}) under enthalpy control. The [3]pseudorotaxane shows a dual function as the monomer of **A** and as the cross-linker, which are essential for hydrogelation. The mixture of α-CD and **1a**Cl ($n = 8$) does not form a hydrogel because the alkyl chain is not long enough for [3]pseudorotaxane formation. Supramolec-

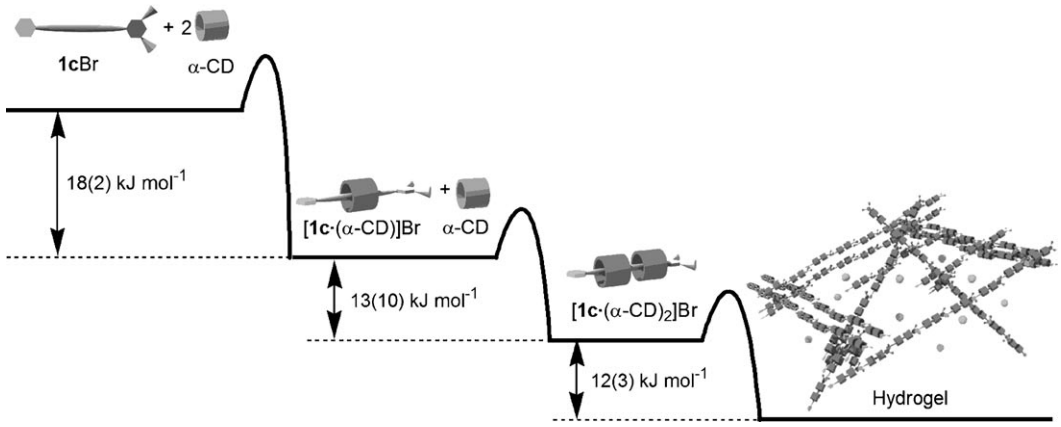

Figure 18. Energy diagram of hydrogelation of **1c**Br and α-CD.

ular polymer **A** is formed by attractive inter-rotaxane interaction between the pyridinium and C_6H_3-3,5-$(OMe)_2$ groups, while it is aggregated by hydrogen bonding between CD molecules.[40,41] Similar cation–π interaction is well known and observed in biological systems.[42] Tsuzuki et al. calculated the interaction energy of the complex of *N*-methylpyridinium and benzene as $-9.36\,kcal\,mol^{-1}$.[43] Fossey et al. reported intramolecular interactions between *N*-methyl pyridinium and benzene by NOE and fluorescence spectroscopy.[44]

Conclusion

We have described facile multicomponent hydrogelation of α-CDs and *N*-alkyl pyridiniums [py-*N*-$(CH_2)_nOC_6H_3$-3,5-$(OMe)_2]^+X^-$. Reaction of **1b**Cl (or **1c**Br) with α-CD in aqueous solution forms [2]- and [3]pseudorotaxanes as an equilibrium mixture, while the reaction of **1a**Cl and α-CD does not give [3]pseudorotaxane but [2]pseudorotaxane. [3]Pseudorotaxanes composed of **1b**Cl (or **1c**Br) and α-CDs aggregate to form supramolecular polymers, followed by entanglement to form three-dimensional networks which immobilize water on the macroscale. Amphiphilic compounds **1b**Cl and **1c**Br form micelles in aqueous solution above their CMCs. During the course of gel formation, solutions of **1b**Cl (or **1c**Br) undergo degradation of the micelle aggregation and afford [3]pseudorotaxanes. They may exist as individual molecules or species and/or supramolecular polymers, which are re-aggregated as the network polymer to form the supramolecular hydrogels. Hydrogel formation was induced by formation of the [3]pseudorotaxane. This unique supramolecular transformation of amphiphiles may provide a new method to control aggregation and functions of these soft materials. Easy construction of supramolecular hydrogels from simple components may provide a new bottom-up approach to the design of biodegradable hydrogels and delivery matrices for drugs.

Experimental Section

Materials and methods: [py-*N*-$(CH_2)_8OC_6H_3$-3,5-$(OMe)_2]^+Cl^-$ (**1a**Cl), [py-*N*-$(CH_2)_{10}OC_6H_3$-3,5-$(OMe)_2]^+Cl^-$ (**1b**Cl), and [py-*N*-$(CH_2)_{12}OC_6H_3$-3,5-$(OMe)_2]^+Br^-$ (**1c**Br) were prepared according to the literature method.[18] Other chemicals were commercially available. NMR spectra (^1H, $^{13}C\{^1H\}$) ware recorded on Varian MERCURY300, Jeol EX-400, and Jeol JNM La-500 spectrometers. ^{13}C CP/MAS NMR spectra were recorded on a JEOL JNM La-500. Sodium 3-(trimethylsilyl)-1-propanesulfonate (DSS) and sodium 3-(trimethylsilyl)-1-propionate (TSP) were used as an external standards in the $^{13}C\{^1H\}$ NMR measurements in D_2O. 2D ROESY spectra were recorded on a JEOL JNM La-500 spectrometer (500 MHz). The parameters used were spin-rock mixing time of 400 ms, PD = 1.2 s, and eight scans. The temperature was kept at 303 K during measurement. Fast atom bombardment mass spectra (FABMS) were obtained with a JEOL JMS-700 spectrometer (2-nitrophenyl *n*-octyl ether (NPOE) or 3-nitrobenzyl alcohol (NBA) matrix). Matrix assisted laser desorption ionization time of flight mass spectra (MALDI-TOFMS) were obtained with a Shimadzu AXIMA-CFR Plus spectrometer (matrix: 2-hydroxy-5-methoxybenzoic acid (super DHB); cationization agent: silver trifluoroacetate). Elemental analysis was carried out with a LECO CHNS-932 CHNS or Yanaco MT-5 CHN autorecorder at the Center for Advanced Materials Analysis, Technical Department, Tokyo Institute of Technology. The absorption spectra were recorded with a Jasco V-530 UV/Vis spectrometer. The samples were stored at a temperature of 25 °C in a Jasco EHC-477 Peltier-type thermostated cell holder prior to measurement. Xerogels were analyzed by scanning electron microscopy (SEM, HITACHI S-5200) at 30 kV. X-ray diffraction (XRD) analyses were carried out with a Rigaku RINT2000.

[py-*N*-$(CH_2)_{10}OC_6H_3$-3,5-$(OMe)_2]^+PF_6^-$ (1bPF$_6$): An aqueous solution (10.0 mL) of **1b**Cl (1.0 g, 2.5 mmol) was poured into an aqueous solution (10.0 mL) of NH_4PF_6 (2.0 g, 12.5 mmol), and the solution was stirred for 21 h at room temperature. The solid product that separated from the mixture was collected by filtration and washed with water to yield **1b**PF_6 as a white solid (1.1 g, 2.1 mmol, 84%). IR (KBr disk, RT): $\tilde{\nu}$ = 839, 558 cm^{-1}; ^1H NMR (400 MHz, [D$_6$]DMSO, RT): δ = 1.20–1.42 (12H, CH_2), 1.65 (m, 2H; OCH_2CH_2), 1.90 (m, 2H; NCH_2CH_2), 3.68 (s, 6H; OCH_3), 3.88 (t, ^3J(H,H) = 6 Hz, 2H; OCH_2), 4.57 (t, ^3J(H,H) = 7 Hz, 2H; NCH_2), 6.05 (3H; C_6H_3), 8.14 (t, ^3J(H,H) = 7 Hz, 2H; C_5H_5N), 8.58 (t, ^3J(H,H) = 8 Hz, 1H; C_5H_5N), 9.06 ppm (d, ^3J(H,H) = 6 Hz, 2H; C_5H_5N); $^{13}C\{^1H\}$ NMR (100 MHz, [D$_6$]DMSO, RT): δ = 25.4 (CH_2), 25.5 (CH_2), 28.3 (CH_2), 28.7 (3C; CH_2), 28.9 (CH_2), 30.7 (CH_2), 55.1 (OCH_3), 60.8 (NCH_2), 67.4 (OCH_2), 92.7 (C_6H_3), 93.1 (C_6H_3), 128.0 (C_5H_5N), 144.5 (C_5H_5N), 145.3 (C_5H_5N), 160.4 (C_6H_3), 161.0 ppm (C_6H_3); MS (FAB): *m/z* calcd for $C_{23}H_{34}NO_3$: 372 $[M-PF_6]^+$; found 372; elemental analysis calcd (%) for $C_{23}H_{34}F_6NO_3P\cdot0.5H_2O$ (517.5): C 52.47, H 6.70, N 2.66; found: C 52.62, H 6.54, N 2.72.

[py-*N*-$(CH_2)_{10}OC_6H_3$-3,5-$(OMe)_2]^+NO_3^-$ (1bNO$_3$): $AgNO_3$ (204 mg, 1.2 mmol) was added to an aqueous solution (10.0 mL) containing **1b**Cl (0.50 g, 1.2 mmol), and the mixture was stirred for 15 h at room temperature in the dark. The formed AgCl was removed by filtration and the product was extracted with acetone (10.0 mL). Evaporation of the solvent under reduced pressure yielded **1b**NO_3 as a white solid (468 mg, 1.1 mmol, 92%). ^1H NMR (400 MHz, [D$_6$]DMSO, RT): δ = 1.19–1.42 (12H; CH_2), 1.65 (m, 2H; OCH_2CH_2), 1.90 (m, 2H; NCH_2CH_2), 3.68 (s, 6H; OCH_3), 3.88 (t, ^3J(H,H) = 6 Hz, 2H; OCH_2), 4.59 (t, ^3J(H,H) = 7 Hz, 2H; NCH_2), 6.05 (3H; C_6H_3), 8.15 (t, ^3J(H,H) = 7 Hz, 2H; C_5H_5N), 8.59 (t, ^3J(H,H) = 7 Hz, 1H; C_5H_5N), 9.09 ppm (d, ^3J(H,H) = 6 Hz, 2H; C_5H_5N); $^{13}C\{^1H\}$ NMR (100 MHz, [D$_6$]DMSO, RT): δ = 25.4 (CH_2), 25.5 (CH_2), 28.4 (CH_2), 28.7 (3C; CH_2), 28.9 (CH_2), 30.7 (CH_2), 55.1 (OCH_3), 60.8 (NCH_2), 67.4 (OCH_2), 92.7 (C_6H_3), 93.1 (C_6H_3), 128.0 (C_5H_5N), 144.6 (C_5H_5N), 145.3 (C_5H_5N), 160.4 (C_6H_3), 161.0 ppm (C_6H_3); elemental analysis calcd (%) for $C_{23}H_{34}N_2O_6\cdot0.5H_2O$ (517.5): C 62.28, H 7.95, N 6.32; found: C 62.38, H 8.21, N 6.41.

[py-*N*-$(CH_2)_{10}OC_6H_3$-3,5-$(OMe)_2]^+[PtCl_3(dmso)]^-$ (1b[PtCl$_3$(dmso)]): An aqueous solution (5.0 mL) of **1b**Cl (0.50 g, 1.3 mmol) was poured into an aqueous solution (10.0 mL) of K[$PtCl_3$(dmso)] (0.60 g, 1.4 mmol), and the solution was stirred for 24 h at room temperature. The formed precipitate was collected by filtration and washed with H_2O, EtOH, and Et_2O to yield **1b**[$PtCl_3$(dmso)] as a yellow solid (0.70 g, 1.0 mmol, 83%). ^1H NMR (300 MHz, [D$_6$]DMSO, RT): δ = 1.18–1.42 (12H; CH_2), 1.64 (br, 2H; OCH_2CH_2), 1.90 (br, 2H; NCH_2CH_2), 2.53 (s, 6H; SCH_3), 3.67 (s, 6H; OCH_3), 3.87 (t, ^3J(H,H) = 6 Hz, 2H; OCH_2), 4.61 (t, ^3J(H,H) = 7 Hz, 2H; NCH_2), 6.04 (3H; C_6H_3), 8.16 (t, ^3J(H,H) = 7 Hz, 2H; C_5H_5N), 8.59 (t, ^3J(H,H) = 7 Hz, 1H; C_5H_5N), 9.09 ppm (d, ^3J(H,H) = 6 Hz, 2H; C_5H_5N); $^{13}C\{^1H\}$ NMR (75.5 MHz, [D$_6$]DMSO, RT): δ = 25.4 (CH_2), 25.5 (CH_2), 28.4 (CH_2), 28.6 (CH_2), 28.7 (2C; CH_2), 28.9 (CH_2), 30.8 (CH_2), 40.3 (SCH_3), 55.1 (OCH_3), 60.8 (NCH_2), 67.4 (OCH_2), 92.7 (C_6H_3), 93.1 (C_6H_3), 128.1 (C_5H_5N), 144.7 (C_5H_5N), 145.5 (C_5H_5N), 160.5 (C_6H_3), 161.1 ppm (C_6H_3); elemental analysis calcd (%) for $C_{25}H_{40}Cl_3NO_4PtS$ (517.5): C 39.92, H 5.36, N 1.86, S 4.26, Cl, 14.14; found: C 39.59, H 5.12, N 1.94, S 4.12, Cl 14.45.

[2]Pseudorotaxane of 1aCl and α-CD ([1a·(α-CD)]Cl): **1a**Cl (53 mg, 0.14 mmol) and α-CD (272 mg, 0.28 mmol) were charged to a NMR tube. After addition of D_2O (0.70 mL) to the mixture, the ^1H NMR spectrum was recorded. The solution contained [**1a**·(α-CD)]Cl and free α-CD. ^1H NMR (400 MHz, D_2O, RT): δ = 1.09–1.51 (8H; CH_2), 1.63 (br, 2H; OCH_2CH_2), 2.00 (br, 2H; NCH_2CH_2), 4.91 (br, 6H; H1-α-CD), 5.83

(2H; C_6H_3), 6.04 (s, 1H; C_6H_3), 7.94 (m, 2H; C_5H_5N), 8.42 (m, 1H; C_5H_5N), 8.77 ppm (m, 2H; C_5H_5N) (peak of NCH_2, OCH_2, OCH_3, H2–6 of α-CD overlapped with the signals of solvent and free α-CD); $^{13}C\{^1H\}$ NMR (100 MHz, D_2O, RT): $\delta = 28.9$ (CH_2), 29.4 (CH_2), 32.1 (CH_2), 32.3 (CH_2), 32.7 (CH_2), 33.9 (CH_2), 58.1 (OCH_3), 62.3 (C6-α-CD), 64.5 (NCH_2), 71.3 (OCH_2), 74.2 (C2-α-CD), 74.6 (C5-α-CD), 76.5 (C3-α-CD), 83.7 (C4-α-CD), 95.2 (C_6H_3), 96.2 (C_6H_3), 104.6 (C1-α-CD), 131.0 (C_5H_5N), 146.6 (C_5H_5N), 148.4 (C_5H_5N), 162.7 (C_6H_3), 163.9 ppm (C_6H_3) (assignment was supported by ^1H–^1H COSY, ^1H–^{13}C COSY, and ROESY spectroscopy in D_2O.); MS (MALDI-TOF): *m/z* calcd for $C_{57}H_{90}NO_{33}$: 1316.5 $[M-Cl]^+$; found 1315.1.

[2]- and [3]pseudorotaxanes of 1bCl and α-CD ([1b·(α-CD)]Cl and [1b·-(α-CD)$_2$]Cl): Compound **1b**Cl (28.6 mg, 7.01×10^{-2} mmol) and α-CD (61.3 mg, 6.31×10^{-2} mmol) were dissolved in D_2O (1.40 mL). Part of the solution was transferred to an NMR tube and ^1H and $^{13}C\{^1H\}$ NMR spectrum were recorded. The resulting mixture showed signals of **1b**Cl (11.1 mM, 22%); [**1b**·(α-CD)]Cl, in which the secondary hydroxyl groups in the α-CD are close proximity to the C_6H_3-3,5-$(OMe)_2$ moiety (32.9 mM, 66%); and isomers of [**1b**·(α-CD)]Cl (5.1 mM, 10%) and [**1b**·(α-CD)$_2$]Cl (0.9 mM, 2%), while signals of free α-CD was not observed. Further addition of α-CD (68.1 mg, 7.01×10^{-2} mmol) to the solution at 60°C and cooling to room temperature gave a hydrogel. ^1H and $^{13}C\{^1H\}$ NMR spectra of the gel showed the presence of [**1b**·(α-CD)]Cl, [**1b**·(α-CD)$_2$]Cl, and free α-CD. The concentrations of the compounds were determined from the peak area ratio of the *ortho*-C_6H_3 proton. ^1H NMR data of [**1b**·(α-CD)]Cl showed that the secondary hydroxyl groups in the α-CD face the C_6H_3-3,5-$(OMe)_2$ moiety (400 MHz, D_2O, RT): $\delta = 1.95$ (m, 2H; NCH_2CH_2), 5.97 (s, 2H; *ortho*-C_6H_3), 6.07 (s, 1H; *para*-C_6H_3); ^1H NMR data of [**1b**·(α-CD)]Cl showed that the primary hydroxyl groups in the α-CD face the C_6H_3-3,5-$(OMe)_2$ moiety (400 MHz, D_2O, RT): $\delta = 1.84$ (m, 2H; NCH_2CH_2), 6.05 (s, 1H; *para*-C_6H_3), 6.13 (s, 2H; *ortho*-C_6H_3); ^1H NMR data of [**1b**·(α-CD)$_2$]Cl (400 MHz, D_2O, RT): $\delta = 1.81$ (br, 2H; NCH_2CH_2), 5.59 (s, 2H; *ortho*-C_6H_3), 6.28 (s, 1H; *para*-C_6H_3); other signals of [**1b**·(α-CD)]Cl and [**1b**·(α-CD)$_2$]Cl were not distinguished from each other due to severe overlap; $\delta = 1.00$–1.59 (14H; CH_2), 3.37–3.85 (44H; CH-α-CD, CH_2-α-CD, OCH_2-axle, OCH_3), 4.51 (t, $^3J(H,H) = 7$ Hz, 2H; NCH_2), 4.92 (d, $^3J(H,H) = 3$ Hz, 6H; H1-α-CD), 7.92 (br, 2H; C_5H_5N), 8.39 (br, 2H; C_5H_5N), 8.74 ppm (br, 2H; C_5H_5N); $^{13}C\{^1H\}$ NMR data of [**1b**·(α-CD)]Cl (100 MHz, D_2O, RT): $\delta = 28.7$ (CH_2), 29.7 (CH_2), 31.9 (CH_2), 32.2 (CH_2), 32.7 (CH_2), 33.4 (CH_2), 33.6 (2C; CH_2), 58.1 (OCH_3), 62.2 (C6-α-CD), 64.4 (NCH_2), 70.6 (OCH_2), 74.2 (C2-α-CD), 74.5 (C5-α-CD), 76.5 (C3-α-CD), 83.7 (C4-α-CD), 95.7 (C_6H_3), 96.5 (C_6H_3), 104.6 (C1-α-CD), 130.8 (C_5H_5N), 146.6 (C_5H_5N), 148.1 (C_5H_5N), 162.5 (C_6H_3), 163.7 ppm (C_6H_3); $^{13}C\{^1H\}$ NMR data of [**1b**·(α-CD)$_2$]Cl (100 MHz, D_2O, RT): $\delta = 62.5$ (α-CD), 63.1 (α-CD), 75.3 (α-CD), 76.7 (α-CD), 83.0 (α-CD), 84.2 ppm (α-CD); other signals significantly overlapped with signals of [**1b**·(α-CD)]Cl and free α-CD. The assignment was supported by ^1H–^1H COSY, ^1H–^{13}C COSY, and ROESY spectroscopy in D_2O); MS (MALDI-TOF) data of [**1b**·(α-CD)]Cl: *m/z* calcd for $C_{61}H_{98}NO_{33}$: 1344.6 $[M-Cl]^+$; found 1344.6; MS (MALDI-TOF) data of [**1b**·(α-CD)$_2$]Cl: *m/z* calcd for $C_{97}H_{158}NO_{63}$: 2316.9 $[M-Cl]^+$; found 2316.7.

[2]- and [3]pseudorotaxanes of 1cBr and α-CD ([1c·(α-CD)]Br and [1c·-(α-CD)$_2$]Br): **1c**Br (6.7 mg, 1.4×10^{-2} mmol) and α-CD (13.6 mg, 1.40×10^{-2} mmol) were charged to an NMR tube. After addition of D_2O (0.70 mL) to the mixture at room temperature, the ^1H NMR spectrum of the resulting mixture contained signals of **1c**Br (6.5 mM, 32%), [**1c**·(α-CD)]Br, in which the secondary hydroxy groups in the α-CD are in close proximity to the C_6H_3-3,5-$(OMe)_2$ moiety (7.7 mM, 39%), [**1c**·(α-CD)]Br, in which the primary hydroxy groups in the α-CD are close to the C_6H_3-3,5-$(OMe)_2$ moiety (1.4 mM, 7%), and [**1c**·(α-CD$_2$]Br (4.4 mM, 22%). Further addition of α-CD (47.7 mg, 4.91×10^{-2} mmol) to the solution led to formation of [**1c**·(α-CD)$_2$]Br as major component. ^1H and $^{13}C\{^1H\}$ NMR spectra of the solution showed the existence of [**1c**·(α-CD)$_2$]Br and free α-CD. The concentration of the compounds was determined from the peak area ratio of the *ortho*-C_6H_3 proton. ^1H NMR data of [**1c**·(α-CD)]Br showed that the secondary hydroxyl groups in the α-CD face the C_6H_3-3,5-$(OMe)_2$ moiety (500 MHz, D_2O, RT): $\delta = 6.04$ (d, $^3J(H,H) = 2$ Hz, 2H; *ortho*-C_6H_3), 6.08 (dd, $^3J(H,H) = 2$, 2 Hz, 1H; *para*-C_6H_3); ^1H NMR data of [**1c**·(α-CD)]Br showed that the primary hydroxyl groups in the α-CD face the C_6H_3-3,5-$(OMe)_2$ moiety (500 MHz, D_2O, RT): $\delta = 6.06$ (dd, $^3J(H,H) = 2$, 2 Hz, 1H; *para*-C_6H_3), 6.12 (d, $^3J(H,H) = 2$ Hz, 2H; *ortho*-C_6H_3); other signals of the isomers of [**1c**·(α-CD)]Br were not distinguished from each other due to severe overlap; $\delta = 1.51$ (m, 2H; OCH_2CH_2), 1.92 (m, 2H; NCH_2CH_2), 3.49 (dd, $^3J(H,H) = 3$, 10 Hz, H2-α-CD), 3.52 (dd, $^3J(H,H) = 9$ Hz, 6H; H4-α-CD), 3.59 (dd, $^3J(H,H) = 3$, 10 Hz, 6H; H5-α-CD), 3.64 (s, 6H; OCH_3), 3.75 (dd, $^3J(H,H) = 9$, 9 Hz, 6H; H3-α-CD), 4.48 (t, $^3J(H,H) = 7$ Hz, 2H; NCH_2), 4.90 (d, $^3J(H,H) = 3$ Hz, 6H; H1-α-CD), 7.89 (t, $^3J(H,H) = 7$ Hz, 2H; C_5H_5N), 8.37 (t, $^3J(H,H) = 7$ Hz, 1H; C_5H_5N), 8.70 ppm (d, $^3J(H,H) = 6$ Hz, 2H; C_5H_5N); ^1H NMR data of [**1c**·(α-CD)$_2$]Br (500 MHz, D_2O, RT): $\delta = 0.92$–1.54 (18H; CH_2), 1.78–1.96 (2H; NCH_2CH_2), 4.48 (br, 2H; NCH_2), 5.63 (s, 2H; *ortho*-C_6H_3), 6.17 (s, 1H; *para*-C_6H_3), 7.99 (br, 2H; C_5H_5N), 8.47 (br, 1H; C_5H_5N), 8.75 ppm (br, 2H; C_5H_5N); the signals of OCH_2, OCH_3, and α-CD of [**1c**·(α-CD)$_2$]Br overlapped significantly with the signal of free α-CD; $^{13}C\{^1H\}$ NMR data of [**1c**·(α-CD)]Br (125 MHz, D_2O, RT): $\delta = 28.4$ (CH_2), 29.4 (CH_2), 31.7 ($2CH_2$), 32.2 (CH_2), 33.3 (CH_2), 33.4 (CH_2), 33.6 (CH_2), 33.7 (CH_2), 34.1 (CH_2), 58.4 (OCH_3), 62.4 (C6-α-CD), 64.8 (NCH_2), 70.8 (OCH_2), 74.5 (C2-α-CD), 74.8 (C5-α-CD), 76.7 (C3-α-CD), 84.1 (C4-α-CD), 96.3 (C_6H_3), 96.8 (C_6H_3), 105.0 (C1-α-CD), 131.1 (C_5H_5N), 147.0 (C_5H_5N), 148.4 (C_5H_5N), 163.0 (C_6H_3), 164.1 ppm (C_6H_3); $^{13}C\{^1H\}$ NMR data of [**1c**·(α-CD)$_2$]Br (125 MHz, D_2O, RT): $\delta = 29.7$ (CH_2), 29.9 (CH_2), 33.2 (CH_2), 33.8 (CH_2), 33.9 (CH_2), 34.1 (CH_2), 34.6 (CH_2), 34.7 (CH_2), 35.0 (CH_2), 35.4 (CH_2), 58.5 (OCH_3), 62.4 (C6-α-CD), 62.9 (C6′-α-CD), 64.7 (NCH_2), 71.6 (OCH_2), 75.1 (C2-α-CD), 74.8 (C5-α-CD), 76.7 (C3-α-CD), 83.4 (C4-α-CD), 94.9 (C_6H_3), 96.4 (C_6H_3), 105.3 (C1-α-CD), 105.4 (C1′-α-CD), 131.3 (C_5H_5N), 147.1 (C_5H_5N), 148.9 (C_5H_5N), 162.7 (C_6H_3), 164.5 ppm (C_6H_3); signals of C2′-, C3′-, C4′-, and C5′-α-CD were significantly overlapped with the signal of free α-CD. The assignment was supported by ^1H–^1H COSY, ^1H–^{13}C COSY, and ROESY spectroscopy in D_2O); MS (MALDI-TOF) data of [**1c**·(α-CD)]Br: *m/z* calcd for $C_{61}H_{98}NO_{33}$: 1372.6 $[M-Br]^+$; found 1373.4; MS (MALDI-TOF) data of [**1c**·(α-CD)$_2$]Br: *m/z* calcd for $C_{97}H_{158}NO_{63}$: 2344.9 $[M-Br]^+$; found 2347.6.

Thermodynamic parameters of [2]- and [3]pseudorotaxane and hydrogel formation

Formation of [1a·(α-CD)]Cl: The equilibrium constants for [**1a**·(α-CD)]Cl formation ($K_1 = [[\mathbf{1a}\cdot(\alpha\text{-CD})]Cl]/[\mathbf{1a}Cl][\alpha\text{-CD}]$) were determined by means of ^1H NMR spectroscopy. **1a**Cl (5.3 mg, 1.4×10^{-2} mmol) and α-CD (6.8 mg, 7.0×10^{-3} mmol) were charged to a NMR tube. After addition of D_2O (1.40 mL) to the mixture, ^1H NMR spectra were recorded at various temperatures (303, 313, 323, 333, and 343 K). The concentration of the **1a**Cl and [**1a**·(α-CD)]Cl at each temperatures were obtained by comparison of ^1H NMR peak area ratio of the signals d and d′. Plotting the natural logarithm of K_1 against reciprocal absolute temperature gave straight lines ($R^2 = 0.99$), which provide ΔH_1° and ΔS_1°.

Formation of [1b·(α-CD)]Cl: The equilibrium constants for [**1b**·(α-CD)]Cl formation ($K_1 = [[\mathbf{1b}\cdot(\alpha\text{-CD})]Cl]/[\mathbf{1b}Cl,\alpha\text{-CD}]$) were determined in a similar way. **1b**Cl (2.9 mg, 7.0×10^{-3} mmol) and α-CD (3.4 mg, 3.5×10^{-3} mmol) were charged to a NMR tube. After addition of D_2O (0.70 mL) to the mixture, ^1H NMR spectra were recorded at various temperatures (308, 313, 333, 343, and 353 K). At each temperature, the signals of [**1b**·(α-CD)$_2$]Cl were not observed. Plotting the natural logarithm of the K_1 against reciprocal absolute temperature gave straight lines ($R^2 = 0.98$), which provide ΔH_1° and ΔS_1°.

Formation of [1b·(α-CD)$_2$]Cl: The equilibrium constants for [**1b**·(α-CD)$_2$]Cl formation ($K_2 = [[\mathbf{1b}\cdot(\alpha\text{-CD})_2]Cl]/[[\mathbf{1b}\cdot(\alpha\text{-CD})]Cl][\alpha\text{-CD}]$) were determined in a similar way. **1b**Cl (20.4 mg, 0.05 mmol) and α-CD (97.3 mg, 0.10 mmol) were charged to a NMR tube. After addition of D_2O (0.70 mL) in the presence of NEt_4Cl (5.0 mM) to the mixture, ^1H NMR spectra were recorded at various temperatures (308, 311, 313, 318, 323, and 328 K). At each temperature, the signals of **1b**Cl were not observed. Plotting the natural logarithm of the K_2 against reciprocal absolute temperature gave straight lines ($R^2 = 0.97$), which provide ΔH_2° and ΔS_2°.

Formation of [1c·(α-CD)]Br: The equilibrium constants for [**1c**·(α-CD)]Br formation ($K_1 = [[\mathbf{1c}\cdot(\alpha\text{-CD})]Br]/[\mathbf{1c}Br][\alpha\text{-CD}]$) were determined

in a similar way. **1c**Br (3.4 mg, 7.0×10^{-3} mmol) and α-CD (3.4 mg, 3.5×10^{-3} mmol) were charged to a NMR tube. After addition of D_2O (0.70 mL) to the mixture, ^1H NMR spectra were recorded at various temperatures (323, 333, 338, and 343 K). At each temperature, the signals of [**1c**·(α-CD)$_2$]Br were not observed. Plotting the natural logarithm of K_1 against reciprocal absolute temperature gave straight lines ($R^2=0.99$), which provide ΔH_1° and ΔS_1°, respectively.

Formation of [1c·(α-CD)$_2$]Br: The equilibrium constants for [**1c**·(α-CD)$_2$]Br formation ($K_2=$[[**1c**·(α-CD)$_2$]Br]/[[**1c**·(α-CD)]Br][α-CD]) were determined by similar may. **1c**Br (1.7 mg, 3.5×10^{-3} mmol) and α-CD (6.8 mg, 7.0×10^{-3} mmol) were charged to a NMR tube. After addition of D_2O (0.70 mL) to the mixture, ^1H NMR spectra were recorded at various temperatures (303, 308, 313, 318, 323, and 328 K). At each temperature, the signals of **1c**Br were not observed. Plotting the natural logarithm of K_2 against reciprocal absolute temperature gave straight lines ($R^2=0.95$), which provide ΔH_2° and ΔS_2°, respectively.

Dissolution of hydrogel of 1cBr and α-CD: Compound **1c**Br (6.7 mg, 1.4×10^{-2} mmol) and α-CD (68.1 mg, 7.0×10^{-2} mmol) were charged to a NMR tube. After addition of D_2O (0.70 mL) in the presence of NBu_4Br (5.0 mM) to the mixture, ^1H NMR spectra were recorded at various temperatures (278, 283, 288, 293, 298, 301, 303, 305, and 308 K). From the known concentration of internal standard and initial concentration of **1c**Br, the concentration of [**1c**·(α-CD)$_2$]Br in solution ([[**1c**·(α-CD)$_2$]Br]$_{(Sol)}$) and that of the gel phase ([[**1c**·(α-CD)$_2$]Br]$_{(gel)}$) were calculated, respectively. At each temperature, the signals of **1c**Br and [[**1c**·(α-CD)]Br were not observed. Plotting the natural logarithm of K_d (=[[**1c**·(α-CD)$_2$]Br]$_{(sol)}$) against reciprocal absolute temperature gave straight lines ($R^2=0.99$), which provide ΔH_d° and ΔS_d°.

Dissolution of hydrogel of 1bCl and α-CD: Compound **1b**Cl (20.4 mg, 5.00×10^{-2} mmol) and α-CD (97.3 mg, 1.00×10^{-1} mmol) were charged to a NMR tube. After addition of D_2O (1.00 mL) in the presence of NEt_4Cl (5.0 mM) to the mixture, ^1H NMR spectra were recorded at various temperatures (293, 296, 289, 303, and 305 K). From the known concentration of internal standard and initial concentration of **1b**Cl, the concentration of **1b**Cl·(α-CD) and **1b**Cl·(α-CD)$_2$ in solution and that of the gel phase were calculated, respectively. K_{d1} and K_{d2} were estimated to be [[**1b**·(α-CD)]Cl]$_{(sol)}$ and [[**1b**·(α-CD)$_2$]Cl]$_{(sol)}$, respectively. At each temperature, the signals of **1b**Cl were not observed. Plotting the natural logarithm of K_{d1} (or K_{d2}) against reciprocal absolute temperature gave straight lines for each compounds ($R^2=0.99$), which provide ΔH_d° and ΔS_d°.

Gelation criterion and determination of sol/gel phase-transition temperatures T_{gel}

Gelation criterion: Stability to inversion of a test tube was used as a general criterion for gel formation.[35] *N*-Alkyl pyridinium, α-CD, and the solvent were put in a septum-capped glass tube (internal diameter/length 18 mm/40 mm) and heated at 60 °C until the solid dissolved. The solution was cooled to room temperature or 0 °C in an ice–water bath. If the gel existed stably, it was classified as a hydrogel. If the sample was a solution, it was classified as a sol.

Gel-to-sol phase transition temperature (T_{gel}): We determined T_{gel} by two methods: stability to inversion of a test tube and the spectroscopic turbidity method.[36] In the former method, a glass tube containing gel was immersed upside-down in a thermostatted bath. In the latter, we prepared the gel in a 10 mm optical cell and measured the transmittance at 600 nm where the *N*-alkyl pyridinium and α-CD do not absorb. Gradually increasing the temperature of the gel leads to gel-to-sol phase transition with no absorption at 600 nm, and this temperature was regarded as T_{gel}.

Reaction of gel with phloroglucinol: Compound **1b**Cl (20.4 mg, 5.0×10^{-2} mmol), α-CD (97.3 mg, 1.0×10^{-1} mmol), and phloroglucinol (25.2 mg, 0.200 mmol) were charged to a glass tube. After addition of D_2O (1.00 mL), the mixture was heated at 60 °C until the solid had dissolved. The solution was cooled to room temperature, and did not form a hydrogel. Part of the solution was transferred to an NMR tube and ^1H NMR and 2D ROESY spectra were recorded.

Acknowledgements

We thank our colleagues in the Chemical Resources Laboratory of Tokyo Institute of Technology for their technical support and discussions; Dr. Yoshiyuki Nakamura for ^{13}C CP/MAS NMR measurements, Dr. Masato Koizumi of the Center for Advanced Materials Analysis, Technical Department, Tokyo Institute of Technology for MALDI-TOF MS measurements, Dr. Daling Lu for scanning electron microscopy (SEM) measurements, and Tomohito Ide for theoretical calculation of the interaction energy of the model complex. This work was supported by a Grant-in-Aid for Scientific Research for Young Scientists from the Ministry of Education, Culture, Sports, Science and Technology, Japan (19750044), and by the Global COE program "Education and Research Center for Emergence of New Molecular Chemistry". T.T. acknowledges the scholarship by the Japan Society for the Promotion of Science.

[1] R. L. Whistler, C. L. Smart, *Polysaccharide Chemistry*, Academic Press, New York, **1953**.
[2] a) K. Akiyoshi, S. Deguchi, N. Moriguchi, S. Yamaguchi, J. Sunamoto, *Macromolecules* **1993**, *26*, 3062–3068; b) N. Morimoto, F. M. Winnik, K. Akiyoshi, *Langmuir* **2007**, *23*, 217–223.
[3] W. Pilnik, F. M. Rombouts, *Carbohydr. Res.* **1985**, *142*, 93–105.
[4] N. A. Peppas, J. Z. Hilt, A. Khademhosseini, R. Langer, *Adv. Mater.* **2006**, *18*, 1345–1360.
[5] a) J. L. Drury, D. J. Mooney, *Biomaterials* **2003**, *24*, 4337–4351; b) S. Ladet, L. David, A. Domard, *Nature* **2008**, *452*, 76–80.
[6] a) Y. Nomura, M. Ikeda, N. Yamaguchi, Y. Aoyama, K. Akiyoshi, *FEBS Lett.* **2003**, *553*, 271–276; b) Y. Nomura, Y. Sasaki, M. Takagi, T. Narita, Y. Aoyama, K. Akiyoshi, *Biomacromolecules* **2005**, *6*, 447–452.
[7] a) R. Valentin, K. Molvinger, F. Quignard, D. Brunel, *New J. Chem.* **2003**, *27*, 1690–1692; b) E. Guibal, *Prog. Polym. Sci.* **2005**, *30*, 71–109; c) D. J. Macquarrie, J. J. E. Hardy, *Ind. Eng. Chem. Res.* **2005**, *44*, 8499–8520; d) M. Chtchigrovsky, A. Primo, P. Gonzalez, K. Molvinger, M. Robitzer, F. Quignard, F. Taran, *Angew. Chem.* **2009**, *121*, 6030–6034; *Angew. Chem. Int. Ed.* **2009**, *48*, 5916–5920.
[8] a) K. Harata, *Chem. Rev.* **1998**, *98*, 1803–1827; b) H.-J. Schneider, F. Hacket, V. Rüdiger, *Chem. Rev.* **1998**, *98*, 1755–1785; c) W. Saenger, J. Jacob, K. Gessler, T. Steiner, D. Hoffmann, H. Sanbe, K. Koizumi, S. M. Smith, T. Takaha, *Chem. Rev.* **1998**, *98*, 1787–1802.
[9] T. Kida, Y. Marui, K. Miyawaki, E. Kato, M. Akashi, *Chem. Commun.* **2009**, 3889–3891.
[10] J. Li, A. Harada, M. Kamachi, *Polym. J.* **1994**, *26*, 1019–1026.
[11] a) Y. Okumura, K. Ito, *Adv. Mater.* **2001**, *13*, 485–487; b) K. Ito, *Polym. J.* **2007**, *39*, 489–499; c) J. Araki, K. Ito, *Soft Matter* **2007**, *3*, 1456–1473.
[12] T. Oku, Y. Furusho, T. Takata, *Angew. Chem.* **2004**, *116*, 984–987; *Angew. Chem. Int. Ed.* **2004**, *43*, 966–969.
[13] C. de Rango, P. Charpin, J. Navaza, N. Keller, I. Nicolis, F. Villain, A. W. Coleman, *J. Am. Chem. Soc.* **1992**, *114*, 5475–5476.
[14] D. Rizkov, S. Mizrahi, J. Gun, R. Hoffman, A. Melman, O. Lev, *Langmuir* **2008**, *24*, 11902–11910.
[15] a) W. Deng, H. Yamaguchi, Y. Takashima, A. Harada, *Angew. Chem.* **2007**, *119*, 5236–5239; *Angew. Chem. Int. Ed.* **2007**, *46*, 5144–5147; b) W. Deng, H. Yamaguchi, Y. Takashima, A. Harada, *Chem. Asian J.* **2008**, *3*, 687–695; c) A. Harada, Y. Takashima, H. Yamaguchi, *Chem. Soc. Rev.* **2009**, *38*, 875–882.
[16] a) A. Miyawaki, Y. Takashima, H. Yamaguchi, A. Harada, *Chem. Lett.* **2007**, *36*, 828–829; b) A. Miyawaki, Y. Takashima, H. Yamaguchi, A. Harada, *Tetrahedron* **2008**, *64*, 8355–8361.
[17] a) L. Zhu, X. Ma, F. Ji, Q. Wang, H. Tian, *Chem. Eur. J.* **2007**, *13*, 9216–9222; b) X. Ma, Q. Wang, D. Qu, Y. Xu, F. Ji, H. Tian, *Adv. Funct. Mater.* **2007**, *17*, 829–837.
[18] T. Taira, Y. Suzaki, K. Osakada, *Chem. Commun.* **2009**, 7027–7029.
[19] a) Y. Suzaki, T. Taira, K. Osakada, *Dalton Trans.* **2006**, 5345–5351; b) Y. Suzaki, T. Taira, K. Osakada, *Transition Met. Chem.* **2007**, *32*, 753–756.

[20] a) Y. Suzaki, T. Taira, D. Takeuchi, K. Osakada, *Org. Lett.* **2007**, *9*, 887–890; b) Y. Suzaki, T. Taira, K. Osakada, M. Horie, *Dalton Trans.* **2008**, 4823–4833.

[21] a) C. Forder, C. S. Patrickios, S. P. Armes, N. C. Billingham, *Macromolecules* **1996**, *29*, 8160–8169; b) D. Takeuchi, A. Inoue, F. Ishimaru, K. Osakada, *J. Polym. Sci. Part A: Polym. Chem.* **2009**, *47*, 959–972.

[22] a) K. Kalyanasundaram, J. K. Thomas, *J. Am. Chem. Soc.* **1977**, *99*, 2039–2044; b) C. B. Roxlo, H. W. Deckman, B. Abeles, *Phys. Rev. Lett.* **1986**, *57*, 2462–2465.

[23] a) T. Okubo, H. Kitano, N. Ise, *J. Phys. Chem.* **1976**, *80*, 2661–2664; b) A. Diaz, P. A. Quintela, J. M. Schuette, A. E. Kaifer, *J. Phys. Chem.* **1988**, *92*, 3537–3542; c) E. Junquera, E. Aicart, G. Tardajos, *J. Phys. Chem.* **1992**, *96*, 4533–4537; d) A. Toki, H. Yonemura, T. Matsuo, *Bull. Chem. Soc. Jpn.* **1993**, *66*, 3382–3386; e) G. M. Nicolle, A. E. Merbach, *Chem. Commun.* **2004**, 854–855; f) E. Mileo, P. Franchi, R. Gotti, C. Bendazzoli, E. Mezzina, M. Lucarini, *Chem. Commun.* **2008**, 1311–1313.

[24] a) C. Park, I. H. Lee, S. Lee, Y. Song, M. Rhue, C. Kim, *Proc. Natl. Acad. Sci. USA* **2006**, *103*, 1199–1203; b) Y. Wang, N. Ma, Z. Wang, X. Zhang, *Angew. Chem.* **2007**, *119*, 2881–2884; *Angew. Chem. Int. Ed.* **2007**, *46*, 2823–2826; c) J. Zou, F. Tao, M. Jiang, *Langmuir* **2007**, *23*, 12791–12794; d) Y. Wang, H. Xu, X. Zhang, *Adv. Mater.* **2009**, *21*, 2849–2864.

[25] a) T. Taira, Y. Suzaki, K. Osakada, *Chem. Lett.* **2008**, *37*, 182–183; b) T. Taira, Y. Suzaki, K. Osakada, *Chem. Asian J.* **2008**, *3*, 895–902.

[26] The pseudorotaxanes in this study may be alternatively termed "semirotaxanes", since supramolecule with a stopper at one end of the axle component are sometimes classified into a subdivision of pseudorotaxanes; a) R. S. Wylie, D. H. Macartney, *J. Am. Chem. Soc.* **1992**, *114*, 3136–3138; b) J.-P. Collin, P. Gaviña, J.-P. Sauvage, *New J. Chem.* **1997**, *21*, 525–528; c) C. Seel, A. H. Parham, O. Safarowsky, G. M. Hübner, F. Vögtle, *J. Org. Chem.* **1999**, *64*, 7236–7242. We prefer to refer to the present supramolecules as "pseudorotaxanes" to avoid confusion and because "pseudorotaxane" is employed more commonly in reports on this area.

[27] For examples of stereoselective synthesis of cyclodextrin[3]rotaxanes, see: a) A. G. Cheetham, T. D. W. Claridge, H. L. Anderson, *Org. Biomol. Chem.* **2007**, *5*, 457–462; b) H. W. Daniell, E. J. F. Klotz, B. Odell, T. D. W. Claridge, H. L. Anderson, *Angew. Chem.* **2007**, *119*, 6969–6972; *Angew. Chem. Int. Ed.* **2007**, *46*, 6845–6848; c) S. Tsuda, J. Terao, Y. Tanaka, T. Maekawa, N. Kambe, *Tetrahedron Lett.* **2009**, *50*, 1146–1150.

[28] a) H. Saito, H. Yonemura, H. Nakamura, T. Matsuo, *Chem. Lett.* **1990**, *19*, 535–538; b) H. Yonemura, M. Kasahara, H. Saito, H. Nakamura, T. Matsuo, *J. Phys. Chem.* **1992**, *96*, 5765–5770; c) M. Hariharan, P. P. Neelakandan, D. Ramaiah, *J. Phys. Chem. B* **2007**, *111*, 11940–11947.

[29] M. V. Rekharsky, Y. Inoue, *Chem. Rev.* **1998**, *98*, 1875–1917.

[30] Kinetically controlled unidirectional pseudorotaxane formation of α-CD and *N*-alkyl pyridinium compounds: a) T. Oshikiri, Y. Takashima, H. Yamaguchi, A. Harada, *J. Am. Chem. Soc.* **2005**, *127*, 12186–12187; b) T. Oshikiri, Y. Takashima, H. Yamaguchi, A. Harada, *Chem. Eur. J.* **2007**, *13*, 7091–7098; c) H. Yamaguchi, T. Oshikiri, A. Harada, *J. Phys. Condens. Matter* **2006**, *18*, S1809-S1816.

[31] For examples of isomerization of pseudorotaxanes containing α-CD and *N*-alkyl pyridinium compounds: a) D. H. Macartney, *J. Chem. Soc. Perkin Trans. 2* **1996**, 2775–2778; b) J. W. Park, H. J. Song, *Org. Lett.* **2004**, *6*, 4869–4872; c) J. W. Park, H. J. Song, Y. J. Cho, K. K. Park, *J. Phys. Chem. C* **2007**, *111*, 18605–18614.

[32] α-CD may undergo weak interaction with C_6H_3-3,5-$(OMe)_2$. For examples of complexation of α-CD with C_6H_5OMe, see: a) I. B. Golovanov, S. M. Zhenodarova, I. G. Tsygankova, *Russ. J. Gen. Chem.* **2006**, *76*, 267–271; b) E. Estrada, I. Perdomo-López, J. J. Torres-Labandeira, *J. Chem. Inf. Comput. Sci.* **2001**, *41*, 1561; c) Q.-X. Guo, S.-H. Luo, Y.-C. Liu, *J. Inclusion Phenom. Mol. Recognit. Chem.* **1998**, *30*, 173–182.

[33] a) P. C. Manor, W. Saenger, *J. Am. Chem. Soc.* **1974**, *96*, 3630–3639; b) M. J. Gidley, S. M. Bociek, *J. Am. Chem. Soc.* **1988**, *110*, 3820–3829.

[34] a) A. Harada, M. Kamachi, *Macromolecules* **1990**, *23*, 2821–2823; b) I. N. Topchieva, A. E. Tonelli, I. G. Panova, E. V. Matuchina, F. A. Kalashnikov, V. I. Gerasimov, C. C. Rusa, M. Rusa, M. A. Hunt, *Langmuir* **2004**, *20*, 9036–9043.

[35] a) Y. He, P. Fu, X, Shen, H. Gao, *Micron* **2008**, *39*, 495–516; b) P. Jara, L. Barrientos, B. Herrera, I. Sobrados, *J. Chil. Chem. Soc.* **2008**, *53*, 1474–1476.

[36] a) J. E. Eldridge, J. D. Ferry, *J. Phys. Chem.* **1954**, *58*, 992–995; b) A. Takahashi, M. Sakai, T. Kato, *Polym. J.* **1980**, *12*, 335–341.

[37] K. Murata, M. Aoki, T. Suzuki, T. Harada, H. Kawabata, T. Komori, F. Ohseto, K. Ueda, S. Shinkai, *J. Am. Chem. Soc.* **1994**, *116*, 6664–6676.

[38] a) J. Makarević, M. Jokić, B. Perić, V. Tomišić, B. Kojić-Prodić, M. Žinić, *Chem. Eur. J.* **2001**, *7*, 3328–3341; b) J. Makarević, M. Jokić, Z. Raza, Z. Štefanić, B. Kojić-Prodić, M. Žinić, *Chem. Eur. J.* **2003**, *9*, 5567–5580; c) D. Rizkov, J. Gun, O. Lev, R. Sicsic, A. Melman, *Langmuir* **2005**, *21*, 12130–121388.

[39] The equilibrium constant of the reaction of [py-*N*-*n*Bu]$^+$(Cl^-) and α-CD was estimated by Benesi–Hildebrand plot to be 21(1) M^{-1}, which is much smaller than those of [**1b**α-CD)]Cl and [**1b**·(α-$CD)_2$]Cl. The effect of complexation of [py-*N*-*n*Bu]$^+$(Cl^-) and α-CD was considerably less significant for the phase transition.

[40] Pseudorotaxanes with channel-type arrangement generally show high crystallinity, which makes the complexes separate from aqueous solutions. [3]Pseudorotaxanes [4,4′-bpy-*N*-$(CH_2)_{10}OC_6H_3$-3,5-$(OMe)_2$·(α-$CD)_2$]$^+Cl^-$ and [py-*N*-$(CH_2)_{15}CH_3$·(α-$CD)_2$]$^+Cl^-$ form crystalline solids, which have a similar structure to **1b**Cl, which suggests that terminal aromatic moiety of axle molecules have significant importance for formation of **A**.[25,41] See also: D.-R. Yei, S.-W. Kuo, H.-K. Fu, F.-C. Chang, *Polymer* **2005**, *46*, 741–750.

[41] Interaction energy of the complex of [py-*N*-Me]$^+$ and C_6H_3-1,3,5-$(OMe)_3$ is calculated to be -19.0 kcal mol^{-1} ($\Delta G = -6.93$ kcal mol^{-1}). See Supporting Information.

[42] a) H. Ritter, F. Koch-Nolte, V. E. Marquez, G. E. Schulz, *Biochemistry* **2003**, *42*, 10155–10162; b) D. T. Major, J. Gao, *J. Am. Chem. Soc.* **2006**, *128*, 16345–16357; c) S. Yamamoto-Katayama, M. Ariyoshi, K. Ishihara, T. Hirano, H. Jingami, K. Morikawa, *J. Mol. Biol.* **2002**, *316*, 711–723; d) B. F. Eichman, E. J. O'Rourke, J. P. Radicella, T. Ellenberger, *EMBO J.* **2003**, *22*, 4898–4909.

[43] S. Tsuzuki, M. Mikami, S. Yamada, *J. Am. Chem. Soc.* **2007**, *129*, 8656–8662.

[44] a) I. Richter, J. Minari, P. Axe, J. P. Lowe, T. D. James, K. Sakurai, S. D. Bull, J. S. Fossey, *Chem. Commun.* **2008**, 1082–1084; b) I. Richter, M. R. Warren, J. Minari, S. A. Elfeky, W. Chen, M. F. Mahon, P. R. Raithby, T. D. James, K. Sakurai, S. J. Teat, S. D. Bull, J. S. Fossey, *Chem. Asian J.* **2009**, *4*, 194–198.

Received: December 3, 2009
Published online: April 21, 2010

